

Isospin–Violating Dark Matter with Colored Mediators

Koichi Hamaguchi^(a,b), Seng Pei Liew^(a),
Takeo Moroi^(a,b) and Yasuhiro Yamamoto^(c)

^a*Department of Physics, University of Tokyo, Bunkyo-ku, Tokyo 113-0033, Japan*

^b*Kavli Institute for the Physics and Mathematics of the Universe, University of Tokyo,
Kashiwa 277-8583, Japan*

^c*Departamento de Física Teórica y del Cosmos, Universidad de Granada,
Granada E-18071, Spain*

Abstract

In light of positive signals reported by the CDMS–II Si experiment and the recent results of the LUX and SuperCDMS experiments, we study isospin–violating dark matter scenarios assuming that the interaction of the dark matter is mediated by colored particles. We investigate the phenomenology of the model, including collider searches, flavor and CP phenomenology. A minimal possible scenario includes scalar dark matter and new vector-like colored fermions with masses of $O(1)$ TeV as mediators. Such a scenario may be probed at the 14 TeV LHC, while flavor and CP constraints are stringent and severe tuning in the couplings is unavoidable. We also found that, as an explanation of the CDMS–II Si signal, isospin–violating fermionic dark matter models with colored scalar mediators are disfavored by the LHC constraints.

1 Introduction

Dark matter (DM), which is expected to be responsible for about 27 % of the mass density of the present universe [1], is still a great mystery to the field of particle physics. Although various cosmological observations have confirmed the existence of DM, its particle-physics properties, such as the mass, strength of its interactions with Standard-Model (SM) particles, and so on, remain fully unknown. Various experiments have been performed to detect direct and indirect signals of DM [2].

In recent years, several direct detection experiments (DAMA/LIBRA [3], CoGeNT [4, 5, 6], CRESST [7] and the CDMS-II Si experiment [8]) have found signals that may suggest the existence of light DM with mass around 10 GeV. On the other hand, experiments such as XENON [9, 10], LUX [11], SIMPLE [12], CDMS [13, 14] and SuperCDMS [15, 16] have not found any excess of events that can be interpreted as signals from DM. In particular, the LUX experiment has probed the relevant region of parameters at the highest level of sensitivity and excluded most regions favored by the possible signals of light DM.

It has been shown that it is difficult to accommodate positive signals of direct detection experiments and bounds from Xenon-based experiments by considering astrophysical alternatives (e.g., modified halo models) or varying assumptions about the Xenon scintillation efficiencies [17, 18, 19]. A scenario that still remains viable in reconciling some of these results is the isospin-violating DM [20, 21, 22, 23, 24, 25, 26]. As different types of nuclei are used in different direct detection experiments, isospin-dependent interactions may happen to interfere destructively for a certain type of nuclei, and thus suppress the DM-nucleus scattering cross section. As LUX experiment [11] currently imposes the most stringent bound on DM, one necessarily considers DM that has negligible interaction with the Xenon nucleus. Recent studies after the LUX result [17, 18, 27, 19] have shown that the isospin-violating DM is still compatible with one of positive signals, those of the CDMS-II Si experiment.

More recently, SuperCDMS Collaboration reported their first result for the WIMP search using their background rejection capabilities [16]. As we shall see, the isospin-violating DM scenario is severely constrained also by SuperCDMS, but there is still a viable region of parameter space.

In this paper, we study a minimal extension of the SM with isospin-violating DM, assuming that the isospin-violating interaction of the DM is mediated by colored particles.¹ We investigate the phenomenology of the model, including collider searches as well as flavor and CP physics, paying particular attention to the parameter region which is consistent with CDMS-Si, LUX and SuperCDMS results. We show that a minimal viable model includes scalar DM and new colored vector-like fermions with masses of $O(1)$ TeV as mediators. The colored vector-like fermions can be tested at the 14 TeV LHC. On the other hand, the flavor and CP constraints severely restrict the parameters of the model. We also show that fermionic DM models with colored scalar mediators are disfavored by the LHC constraints.

¹For recent studies on DM models with colored mediators, see, e.g., Refs. [28, 29, 30, 31, 32].

The remaining of the paper is organized as follows. In Section 2, we study effective operators involving SM and DM fields that reproduce the direct detection experimental results. We then study bounds on these operators from collider search and indirect detection. In Section 3, we introduce a simple model involving only DM and colored mediators as new particles, that can reproduce the effective operators studied in Section 2. We study the current bound (8 TeV LHC) on the colored mediators and their prospects of discovery for 14 TeV LHC. In Section 4, we examine flavor and CP constraints on this model. Section 5 is devoted to conclusions. In Appendix A, we briefly discuss models of isospin-violating fermionic DM mediated by colored scalars.

2 Effective Operators of Isospin-Violating Dark Matter

2.1 Direct detection

We study the case in which the DM interaction is dominated by spin-independent interaction.² In the non-relativistic limit, the elastic scattering cross section of DM with a nucleus composed of Z protons and $(A - Z)$ neutrons can be represented as

$$\sigma_A \simeq \frac{\mu_A^2}{4\pi m_{\text{DM}}^2} [f_p Z + f_n (A - Z)]^2, \quad (1)$$

where $\mu_A = m_A m_{\text{DM}} / (m_A + m_{\text{DM}})$ is the reduced mass, m_A is the mass of the nucleus and m_{DM} is the mass of the DM. f_n and f_p parametrize the coupling between DM and neutron and proton, respectively. Their explicit forms in terms of Lagrangian parameters are shown in the following subsections. An isospin-conserving interaction corresponds to $f_n = f_p$. If the isospin is violated and the ratio of the couplings satisfy a relation $f_n/f_p \simeq -Z/(A - Z)$, the cross section σ_A is suppressed. In particular, the DM–Xenon interaction is suppressed for $f_n/f_p \simeq -0.7$.

Given the very severe bound from LUX experiment, it is important to include the effects of multiple isotopes [24], which leads to

$$\sigma_A = \frac{1}{4\pi m_{\text{DM}}^2} \sum_i \eta_i \mu_{A_i}^2 [f_p Z + f_n (A_i - Z)]^2, \quad (2)$$

where η_i is the natural abundance of the i -th isotope. Results of direct detection experiments are often quoted in terms of “normalized-to-nucleon cross section,” which is given by

$$\sigma_N^{(Z)} = \frac{\mu_p^2}{\sum_i \eta_i \mu_{A_i}^2 A_i^2} \sigma_A = \frac{\sum_i \eta_i \mu_{A_i}^2 [Z + (f_n/f_p)(A_i - Z)]^2}{\sum_i \eta_i \mu_{A_i}^2 A_i^2} \sigma_p. \quad (3)$$

²It is difficult to interpret the CDMS-Si signal as spin-dependent scattering of isospin-violating DM [33].

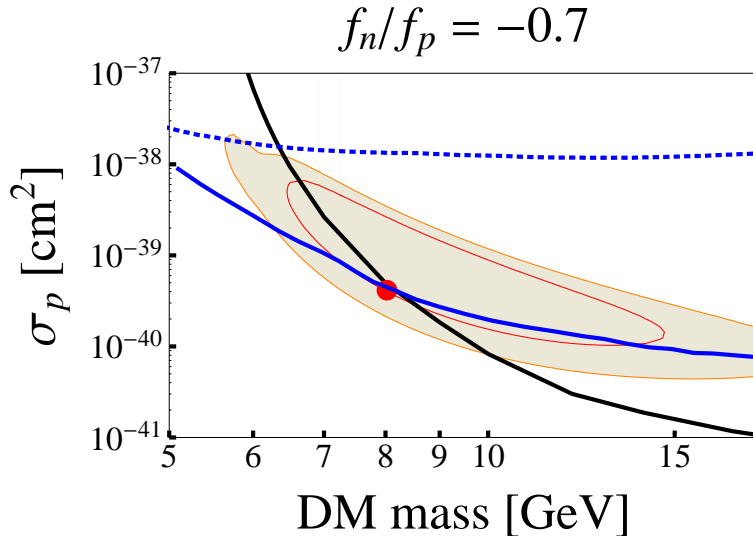


Figure 1: Favored and excluded regions in isospin-violating DM with $f_n/f_p = -0.7$. Shaded regions show 68% and 90% confidence level contours for a possible signal from the CDMS-Si result [8]. Black solid, blue dashed, and blue solid lines represent the exclusion contours from LUX [11], CDMSlite [15], and the recent SuperCDMS [16] experiments, respectively. The red point represent the benchmark point used in our analysis.

In the isospin conserving case, $f_n = f_p$, this is equal to DM-proton cross section σ_p . The DM-Xenon scattering cross section is minimized for $f_n/f_p \simeq -0.7$.

In Fig. 1, we show the parameter regions in $(m_{\text{DM}}, \sigma_p)$ plane for $f_n/f_p = -0.7$, which are favored by CDMS-Si, and excluded by LUX and SuperCDMS.³ In the following analysis, we consider the following representative point of isospin-violating DM:

$$m_{\text{DM}} = 8 \text{ GeV}, \sigma_p = 4 \times 10^{-40} \text{ cm}^2, f_n/f_p = -0.7. \quad (4)$$

One can see that this point is marginally allowed by LUX and SuperCDMS, and is favored by CDMS-Si.

2.2 Effective interactions between quarks and dark matter

The particle DM can be a real or complex scalar field ϕ (and ϕ^* if complex). It can also be a Majorana or a Dirac fermion χ . Assuming that the scattering with nucleon is dominated by spin-independent interaction, there exist only six effective operators at the quark level

³Among many direct detection experimental results, we show in Fig. 1 only positive signals from CDMS-Si and bounds from LUX and SuperCDMS. This is because LUX and SuperCDMS give the most stringent constraints on isospin-violating DM with $f_n/f_p = -0.7$, and only CDMS-Si has significant region of parameters that is not excluded by these bounds.

DM	operator \mathcal{O}	f_N
real	$\mathcal{O}^{(R)} \equiv \sum_{q=u,d} C_q^{(R)} \frac{1}{2} \phi^2 \cdot \bar{q}q$	$\sum_{q=u,d} B_q^{(N)} C_q^{(R)}$
complex (S)	$\mathcal{O}^{(Cs)} \equiv \sum_{q=u,d} C_q^{(Cs)} \phi^* \phi \cdot \bar{q}q$	$\sum_{q=u,d} B_q^{(N)} C_q^{(Cs)}$
complex (V)	$\mathcal{O}^{(Cv)} \equiv \sum_{q=u,d} C_q^{(Cv)} i(\phi^* \partial_\mu \phi - \phi \partial_\mu \phi^*) \bar{q} \gamma^\mu q$	$2m_{\text{DM}} \times \begin{cases} 2C_u^{(Cv)} + C_d^{(Cv)} & (f_p) \\ C_u^{(Cv)} + 2C_d^{(Cv)} & (f_n) \end{cases}$
Majorana	$\mathcal{O}^{(M)} \equiv \sum_{q=u,d} C_q^{(M)} \frac{1}{2} \bar{\chi} \chi \cdot \bar{q}q$	$2m_{\text{DM}} \sum_{q=u,d} B_q^{(N)} C_q^{(M)}$
Dirac (S)	$\mathcal{O}^{(Ds)} \equiv \sum_{q=u,d} C_q^{(Ds)} \bar{\chi} \chi \cdot \bar{q}q$	$2m_{\text{DM}} \sum_{q=u,d} B_q^{(N)} C_q^{(Ds)}$
Dirac (V)	$\mathcal{O}^{(Dv)} \equiv \sum_{q=u,d} C_q^{(Dv)} \bar{\chi} \gamma_\mu \chi \cdot \bar{q} \gamma^\mu q$	$2m_{\text{DM}} \times \begin{cases} 2C_u^{(Dv)} + C_d^{(Dv)} & (f_p) \\ C_u^{(Dv)} + 2C_d^{(Dv)} & (f_n) \end{cases}$

Table 1: Effective operators of quark–DM interactions.

as listed in Table 1.⁴ In this section, we consider only the couplings of DM to up- and down-type quarks, since they give the dominant isospin–violating effects. In the table, we also express the parameters f_n and f_p in terms of the effective couplings C_q , where $B_q^{(N)} = \langle N | \bar{q}q | N \rangle = m_N f_{T_q^{(N)}} / m_q$ ($N = p, n$) are neutron and proton scalar matrix elements. In our numerical analysis, we use the following values: $B_d^{(p)} / B_u^{(p)} = B_u^{(n)} / B_d^{(n)} = 0.80$ [34] and $B_u^{(p)} + B_d^{(p)} = B_u^{(n)} + B_d^{(n)} = 2\sigma_{\pi N} / (m_u + m_d)$ with π -nucleon sigma term $\sigma_{\pi N} \simeq 64$ MeV [34] and light quark mass $(m_u + m_d) / 2 \simeq 3.5$ MeV [35].

In order to reproduce the DM–nucleon cross section of the representative point in Eq. (4), the effective couplings C_q in Table 1 for each scenario are determined as:

$$C_u^{(R,Cs)} \simeq -1.04 \times C_d^{(R,Cs)} \simeq (68 \text{ TeV})^{-1}, \quad (5)$$

$$C_u^{(M,Ds)} \simeq -1.04 \times C_d^{(M,Ds)} \simeq (1050 \text{ GeV})^{-2}, \quad (6)$$

$$C_u^{(Cv,Dv)} \simeq -1.13 \times C_d^{(Cv,Dv)} \simeq (720 \text{ GeV})^{-2}. \quad (7)$$

2.3 LHC bounds on the effective operators

The DM–SM effective operator approach applied to collider physics has been useful in complementing direct and indirect probes of DM [36, 37, 38, 39, 40, 41, 42, 43]. When the DM production at colliders is accompanied by a jet from initial state radiation, the

⁴In the present scenario, the energy scales relevant for collider physics, dark matter detection, and CP / flavor physics are different. In our calculation, however, renormalization group effects on the Wilson coefficients are neglected.

signature will be a jet (mono-jet) with missing transverse energy (MET). The ATLAS and CMS collaborations have also performed searches on mono-photon plus MET, mono-lepton and mono- W or $-Z$ plus MET. These searches currently provide the most stringent collider bounds on DM [44, 45, 46, 47, 48, 49, 50]. To see how severely the isospin-violating DM model is constrained by the LHC data, we have calculated the cross section for these processes. Here, we assume that one of the operators listed in Table 1 dominates the signal process.

For the mono- W and $-Z$ events, our analysis is based on the ATLAS study given in Ref. [50], which utilizes the hadronic decay modes of W and Z boson. We have generated the signal events using MADGRAPH 5 [51], assuming the existence of one of the operators given in Table 1. We apply, in accord with [50], the following cuts at the parton level:

- $p_T^{W,Z} > 250$ GeV, where $p_T^{W,Z}$ is the transverse momentum of W or Z ,
- $|\eta|^{W,Z} < 1.2$, where $\eta^{W,Z}$ is the pseudo-rapidity,
- $\sqrt{y} > 1.2$, where $\sqrt{y} = \min(p_{T1}, p_{T2})\Delta R/m_{\text{jet}}$, with p_{Ti} ($i = 1$ or 2) being the transverse momentum of jet from the decay of W or Z , ΔR the distance between jets, and m_{jet} the calculated mass of the jet.

The fiducial efficiency (63 %) has been taken into account as well. Upper bounds on the dimensionful couplings of the effective operators in Table 1 are obtained based on the observed upper limits on the cross section at 95 % CL in Ref. [48].

We have also calculated the cross section for the mono-jet events. (For the mono-jet bounds on isospin-violating DM, see also [52, 26].) To make a comparison with the ATLAS mono-jet search at 7 TeV [48],⁵ we calculate the parton-level cross section with the following cuts on the mono-jet momentum:

- $p_T > 80$ GeV,
- $|\eta| < 2.0$.

The parton-level cross section is multiplied by the signal acceptance. (Here, we also include the efficiency of the detector, which is taken to be 83 % [48].) In [48], the signal acceptance for the cases with $\mathcal{O}^{(R)}$, $\mathcal{O}^{(Cs)}$, $\mathcal{O}^{(M)}$ and $\mathcal{O}^{(Ds)}$ are not presented. For these cases, we use the acceptance for D5 model given in [48]. (Notice that the scalar interactions considered in [48], i.e., D1 model, are proportional to the quark masses and the effect of c -quark is important. Thus, we do not use the acceptance of the D1 model in our analysis.) We found that, among several signal regions [48], the one corresponding to $p_T > 350$ GeV (SR3) gives the most stringent bounds to the present model. Comparing our estimations of the cross sections with the observed 95 % CL limit on the “visible cross section” given in [48], we derive upper bounds on the coefficients of the effective operators listed in Table 1.

⁵Results at 8 TeV [49] do not have significant improvements compared to the limits obtained in [48].

Effective operator	mono- W or Z	mono-jet
$C_u^{(R)}$	$(630 \text{ GeV})^{-1}$	$(400 \text{ GeV})^{-1}$
$C_u^{(Cs)}$	$(890 \text{ GeV})^{-1}$	$(570 \text{ GeV})^{-1}$
$C_u^{(M)}$	$(820 \text{ GeV})^{-2}$	$(470 \text{ GeV})^{-2}$
$C_u^{(Ds)}$	$(970 \text{ GeV})^{-2}$	$(560 \text{ GeV})^{-2}$
$C_u^{(Cv)}$	$(760 \text{ GeV})^{-2}$	$(430 \text{ GeV})^{-2}$
$C_u^{(Dv)}$	$(1100 \text{ GeV})^{-2}$	$(610 \text{ GeV})^{-2}$

Table 2: Upper bounds on the coefficients of the effective operators obtained from mono- W or $-Z$ and mono-jet searches.

The bounds are given in Table 2. Here, we show the results based on the mono- W and Z events and mono-jet events separately. We can see that the mono- W and $-Z$ processes impose more stringent constraints than the mono-jet process. One of the reasons is that in the isospin-violating DM model, there exists the relative minus sign between the coupling of DM to u - and d -quarks; it results in a constructive interference between two Feynman diagrams for the mono- W production process that greatly enhances the cross section [43].

Comparing Eqs. (5)–(7) with Table 2, the CDMS-Si point with the vector-type effective operators $\mathcal{O}^{(Cv)}$ and $\mathcal{O}^{(Dv)}$ are disfavored. On the other hand, scalar-type interactions, $\mathcal{O}^{(R)}$, $\mathcal{O}^{(Cs)}$, $\mathcal{O}^{(M)}$ and $\mathcal{O}^{(Ds)}$, are still viable. In the next section we introduce a simple model which can reproduce the effective operators $\mathcal{O}^{(R)}$ and $\mathcal{O}^{(Cs)}$ at low energy. (For fermionic DM with effective operators $\mathcal{O}^{(M)}$ and $\mathcal{O}^{(Ds)}$, see Appendix A.)

Before closing this section, let us comment on the validity of the effective field theory (EFT) approach. The effective operators at low energy are generated by a UV theory, typically by exchanges of heavy mediators. At the LHC, the energy scale of the process can be comparable to or larger than the scale of the UV theory. In such a case, the bound obtained by using EFT may not be valid [53, 54, 55, 28, 29, 30, 31, 56, 32]. However, when the effective operators are induced by exchanges of heavy colored mediators, the bound obtained by EFT is typically weaker than the bound obtained by concrete UV models, i.e., EFT gives conservative bounds [32]. Thus, we consider the constraints obtained in this subsection as conservative ones, and discuss UV models for the operators which are not disfavored at the level of EFT.

2.4 Thermal abundance and indirect search

Another important check point is the relic abundance. Although we have assumed the correct DM abundance, the thermal relic density in our model is larger than the present DM density. The thermal relic density is determined by the thermally-averaged pair

Operator	$\langle\sigma_{\text{ann}}v_{\text{rel}}\rangle$	value
$\mathcal{O}^{(\text{R})}$	$3\sum_q C_q^{(\text{R})} ^2/4\pi$	0.04 pb
$\mathcal{O}^{(\text{Cs})}$	$3\sum_q C_q^{(\text{Cs})} ^2/8\pi$	0.02 pb
$\mathcal{O}^{(\text{Dv})}$	$3\sum_q C_q^{(\text{Dv})} ^2 m_{\text{DM}}^2/2\pi$	0.08 pb

Table 3: Thermally averaged total pair annihilation cross sections for the cases with the operators $\mathcal{O}^{(\text{R})}$, $\mathcal{O}^{(\text{Cs})}$, and $\mathcal{O}^{(\text{Dv})}$. For other cases, the cross sections are p -wave suppressed, and are much smaller.

annihilation cross section $\langle\sigma_{\text{ann}}v_{\text{rel}}\rangle$ as

$$\Omega_{\text{thermal}} \simeq 0.2 \times \left(\frac{\langle\sigma_{\text{ann}}v_{\text{rel}}\rangle}{1 \text{ pb}} \right)^{-1}. \quad (8)$$

We show $\langle\sigma_{\text{ann}}v_{\text{rel}}\rangle$ in Table 3 for the cases where the s -wave annihilation processes dominate. (For other cases, the annihilation is via p -wave processes, with which the cross sections are much smaller.) Substituting the cross sections in the table into Eq. (8), we can see that Ω_{thermal} becomes larger than the present density parameter of DM. Thus, we need to consider non-thermal production of DM at $T \ll m_{\text{DM}}$ in the present scenario.

We also comment on the upper bound on $\langle\sigma_{\text{ann}}v_{\text{rel}}\rangle$ from the observations of Milky-Way satellites by Fermi Large Area Telescope (LAT) [57, 58, 52, 59]. With the latest analysis of the γ -ray flux from the satellites [59], the observed upper bound on the pair annihilation cross section into $u\bar{u}$ or $d\bar{d}$ final state is about 0.8 pb for $m_{\text{DM}} = 10$ GeV. As one can see in Table 3, the annihilation cross section in the present model is an order of magnitude smaller than the Fermi-LAT bound.

3 Colored Mediators of Isospin–Violating Dark Matter

As we have seen in the previous section, isospin–violating DM with scalar–type interaction can explain the possible CDMS-Si signal while avoiding the LUX and SuperCDMS constraints as well as the LHC mono–jet and mono– W/Z constraints. In this section we discuss the UV completion of the scalar–type effective couplings. In particular, as mentioned in Introduction, we concentrate on the case that the effective operators are induced by exchanges of heavy colored particles, since they can easily accommodate isospin–violating interactions. For recent studies on other possibilities of isospin–violating DM models, see, for example, [60, 61, 62].

As shown in Appendix A, fermionic DM models require a light colored scalar with a mass smaller than $O(500)$ GeV, and such a model is already excluded by LHC squark search [63]. Thus, in the following discussion, we concentrate on real and complex scalar DM.

particles	$SU(3)_c \times SU(2)_L \times U(1)_Y$	Z_2
ϕ	$(1, 1)_0$	—
$Q (\ni Q_L, Q_R)$	$(3, 2)_{1/6}$	—
$U (\ni U_L, U_R)$	$(3, 1)_{2/3}$	—
$D (\ni D_L, D_R)$	$(3, 1)_{-1/3}$	—
q_L	$(3, 2)_{1/6}$	+
u_R	$(3, 1)_{2/3}$	+
d_R	$(3, 1)_{-1/3}$	+

Table 4: Quantum numbers of DM, colored mediators Q , U , and D (and SM quarks q_L , u_R , and d_R).

3.1 Model

We introduce extra vector-like quarks Q , U , and D , which mediate the coupling between scalar DM and the SM quarks. The matter content and their quantum numbers are summarized in Table 4. (We also list the SM quarks to fix the notation.) We impose a Z_2 symmetry to ensure the stability of DM. The mass and interaction terms of the new colored fields are given by

$$\begin{aligned}
-\mathcal{L}_{Q,U,D} = & M_Q \bar{Q}Q + M_U \bar{U}U + M_D \bar{D}D \\
& + \left(\lambda_Q^i \phi \bar{q}_L^i P_R Q + \lambda_U^i \phi \bar{u}_R^i P_L U + \lambda_D^i \phi \bar{d}_R^i P_L D \right. \\
& + y_{U_L} H_a^\dagger \bar{Q}_a P_L U + y_{D_L} \epsilon^{ab} H_a \bar{Q}_b P_L D \\
& \left. + y_{U_R} H_a^\dagger \bar{Q}_a P_R U + y_{D_R} \epsilon^{ab} H_a \bar{Q}_b P_R D + \text{H.c.} \right). \tag{9}
\end{aligned}$$

The index i stands for the generation of SM quarks. Note that Yukawa couplings between colored mediators and Higgs field is necessary in order to induce a scalar type effective operator between DM and SM quarks, $\mathcal{L}_{\text{eff}} \sim \phi \phi \bar{q} q$. Therefore, after the electroweak symmetry is broken, the two up-type colored mediators mix with a mass matrix

$$\mathcal{M}_U = \begin{pmatrix} M_U & y_{U_L}^* v \\ y_{U_R} v & M_Q \end{pmatrix}, \tag{10}$$

where $v \simeq 174$ GeV is the Higgs vacuum expectation value. The two down-type mediators also mix in a similar way.

In the case of complex scalar DM, we impose a global $U(1)$ symmetry, where only the DM and colored mediators are charged; the Lagrangian (9) has such a symmetry. As we will see, this $U(1)$ symmetry makes phenomenology of complex scalar DM and real one different.

In general, DM can couple to all three generations of SM quarks. In addition, there are CP phases of the couplings in Eq. (9) which cannot be removed by field redefinitions. These

flavor-changing and CP-violating couplings are severely constrained. We will discuss these issues in detail in Section 4. In this and next subsection, we assume that the couplings to the first generation are dominant, and neglect the effects of the couplings to the second and third generations. (We will omit the generation index i from the coupling constants to the first generation quarks until Section 4.3.) For the study of the signals at LHC, for simplicity, we take the following parametrization:

$$M_Q = M_U = M_D \equiv M, \quad (11)$$

$$\lambda_Q = \lambda_U = \lambda_D \equiv \lambda, \quad (12)$$

$$y_{U_L} = y_{U_R} \equiv y_U, \quad (13)$$

$$y_{D_L} = y_{D_R} \equiv y_D, \quad (14)$$

where all parameters are taken to be real. Then, the effective coupling constants in Table 1 are given by

$$C_u^{(R)} = \frac{2\lambda^2 y_U v}{M^2 - y_U^2 v^2}, \quad C_d^{(R)} = \frac{2\lambda^2 y_D v}{M^2 - y_D^2 v^2}, \quad C_u^{(Cs)} = \frac{\lambda^2 y_U v}{M^2 - y_U^2 v^2}, \quad C_d^{(Cs)} = \frac{\lambda^2 y_D v}{M^2 - y_D^2 v^2}. \quad (15)$$

In our analysis, we take $C_u^{(R,Cs)} \simeq (68 \text{ TeV})^{-1}$ (see Eq. (5)). In Fig. 2, on (M, λ) plane, we show contours on which we obtain $C_u^{(R,Cs)} = (68 \text{ TeV})^{-1}$, taking $y_U = 0.1$ and 1. As one can see, the masses of the vector-like quarks must be $O(1)$ TeV as far as all the coupling constants are within the perturbative regime.

3.2 Direct production of colored mediators at LHC

Now we are at the position to discuss the LHC constraints/prospects of the colored mediators. In the present scenario, colored mediators are pair-produced at LHC. Here, there is an important difference between the real and complex scalar DM scenarios. In the former case, the processes $pp \rightarrow Q\bar{Q}$ and QQ both occur, where Q collectively denotes colored mediators while \bar{Q} is the anti-particles. In the case of complex scalar DM, on the contrary, $pp \rightarrow QQ$ is forbidden, so that the relevant processes are only the pair production of Q and \bar{Q} . Notice that the amplitudes with t -channel exchange of DM can enhance the cross section in the present scenario.

Once produced, the colored mediators decay into the SM quarks and the DM particle, so the important processes are ⁶

$$pp \rightarrow \begin{cases} Q\bar{Q} \rightarrow q\phi^{(*)} \bar{q}\phi, \\ QQ \rightarrow q\phi q\phi \quad (\text{only for real scalar DM}), \\ \bar{Q}\bar{Q} \rightarrow \bar{q}\phi \bar{q}\phi \quad (\text{only for real scalar DM}), \end{cases} \quad (16)$$

⁶ The process $pp \rightarrow Q\phi + j$ also contributes to the events with two jets plus missing energy. Transverse momenta of the emitted jets tend to be smaller than that given by the pair productions in this process. Therefore, the contribution becomes sub-dominant with tighter p_T cuts used in Ref. [63]. Since we have neglected these processes, the above bounds are conservative.

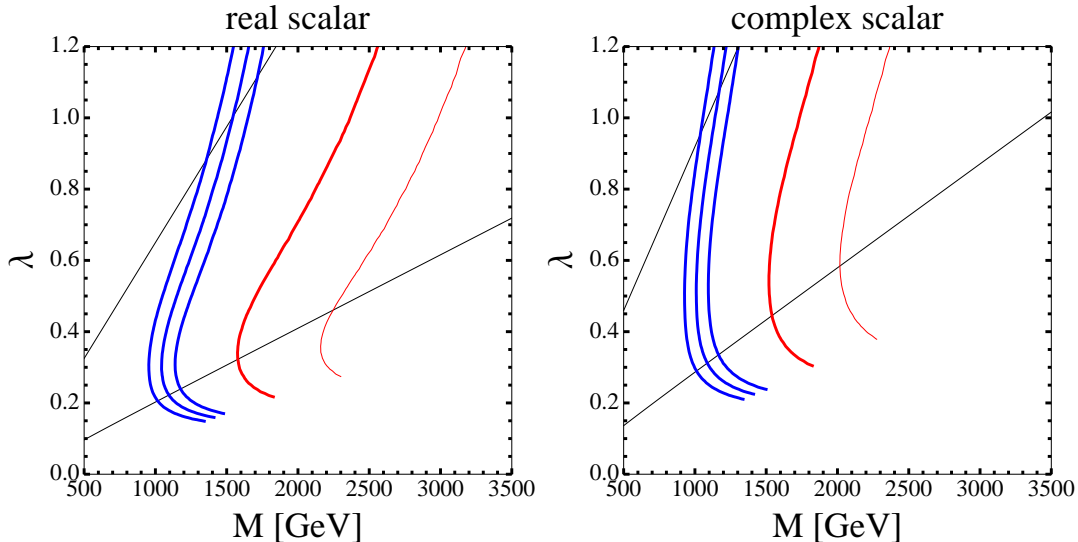


Figure 2: Contour of the total cross section σ_{tot} for the pair production of colored mediators, at leading order in (M, λ) plane, for real and complex scalar DM. Blue lines show the contours of $\sigma_{\text{tot}} = 0.02, 0.01, \text{ and } 0.005$ pb at $\sqrt{s} = 8$ TeV from the left to right. Red lines show the contours of $\sigma_{\text{tot}} = 0.01$ and 0.001 pb at $\sqrt{s} = 14$ TeV from the left to right. Note that Yukawa couplings y_U and y_D are adjusted through Eqs. (15), in order to reproduce the direct detection cross section. Two black solid lines in each figure show the contours of $y_U = 0.1$ and 1 from top to bottom.

where q denotes SM quarks while \bar{q} is its anti-particle. Thus, the LHC signal is two jets plus missing energy. In Fig. 2, we show the contour of total cross section σ_{tot} for the pair production of the colored mediators for $\sqrt{s} = 8$ TeV, where σ_{tot} is calculated by MADGRAPH 5 [51] at the leading-order and is given by

$$\sigma_{\text{tot}} = \begin{cases} \sigma(pp \rightarrow Q\bar{Q}) + \sigma(pp \rightarrow QQ) + \sigma(pp \rightarrow \bar{Q}\bar{Q}) & : \text{ real scalar DM,} \\ \sigma(pp \rightarrow Q\bar{Q}) & : \text{ complex scalar DM.} \end{cases} \quad (17)$$

The di-jet signal with missing energy is studied both at ATLAS and CMS, particularly in the context of supersymmetric (SUSY) models. In the ATLAS analysis [63], a simplified SUSY model is studied, where only first two generation squarks and the lightest neutralino are potentially accessible to LHC while all other SUSY particles (including the gluino) are heavy. In such a model, the lower bound on the common squark mass is 780 GeV, corresponding to the leading-order squark production cross section of 0.013 pb. In general, this value cannot be directly compared with the prediction of the present model because the signal efficiency (i.e., the fraction of signal events which pass the cuts in Ref. [63]) may be different. By using the parton-level analysis with MADGRAPH 5 [51], we estimated the efficiency for our model as well as that for the simplified SUSY model with a squark mass of 780 GeV. Then, we found that the former is comparable to or larger than the

latter. Thus, we translate the ATLAS constraint on the simplified SUSY model to derive a conservative bound on the present model; assuming that σ_{tot} should be smaller than ~ 0.01 pb and $O(1)$ couplings $\lambda, y \lesssim 1$, M is bounded from below as $M \gtrsim 1 - 1.5$ TeV ($1 - 1.1$ TeV) for real (complex) scalar DM, depending on the coupling λ .

Before closing this section, let us discuss the future prospects of the present model. In Fig. 2, we also show the contour of σ_{tot} at $\sqrt{s} = 14$ TeV. At 14 TeV LHC the sensitivity of the search with two-jets plus missing energy may reach $O(0.003)$ pb and $O(0.001)$ pb or larger, for the integrated luminosities of 300 fb^{-1} and 3000 fb^{-1} , respectively [64]. One can see that a large region of the parameter space, possibly above $M \simeq 3$ TeV (2 TeV) for the case of real (complex) scalar DM, may be covered at 14 TeV LHC.

4 Flavor and CP Constraints

In the previous section, we have discussed the LHC phenomenology of the isospin-violating DM model with colored mediators. In the present scenario, the interaction of DM may significantly affect flavor and CP observables, which give very stringent constraints on the present model. We concentrate on the case with scalar DM, since isospin-violating fermionic DM with colored mediators is stringently constrained by the the LHC bounds, as shown in Appendix A.

4.1 Up- and down-quark masses

First we discuss the radiative correction to the SM Yukawa coupling constants in the present model. In particular, we concentrate on the Yukawa coupling constants of up- and down-quarks (which we denote y_u and y_d) on which the corrections are the most significant.

If y_{U_L} or y_{D_L} is non-vanishing, there exist logarithmically-divergent 1-loop contributions to y_u or y_d . Then, the β -functions of the up- and down-quark Yukawa coupling constants become

$$\frac{dy_u}{d \log \mu} = \frac{1}{8\pi^2} \lambda_Q \lambda_U y_{U_L} + \dots, \quad (18)$$

$$\frac{dy_d}{d \log \mu} = \frac{1}{8\pi^2} \lambda_Q \lambda_D y_{D_L} + \dots, \quad (19)$$

where μ is the renormalization scale and “ \dots ” are terms proportional to y_u or y_d . The important point is that the β -functions contain terms which are not proportional to the SM Yukawa coupling constants. Consequently, the smallness of y_u and y_d may be affected in particular when the coupling constants in the DM sector are relatively large. As shown in the previous section, the present scenario requires large values of $\lambda_{Q,U,D}$ and $y_{U,D}$ (cf. Fig. 2). Thus, we expect significant contribution to the up- and down-quark Yukawa coupling constants from the DM sector.

The low-energy values of the Yukawa coupling constants, which are directly related to the up- and down-quark masses, are given by

$$y_u(\mu \ll M_Q) \sim y_u(M_*) + \frac{1}{8\pi^2} \lambda_Q \lambda_U y_{U_L} \log \frac{M_Q}{M_*} + \dots, \quad (20)$$

$$y_d(\mu \ll M_Q) \sim y_d(M_*) + \frac{1}{8\pi^2} \lambda_Q \lambda_D y_{D_L} \log \frac{M_Q}{M_*} + \dots, \quad (21)$$

where M_* is the cut-off scale at which the boundary conditions are given. If $\lambda_{Q,U,D} \sim y_{U_L,D_L} \sim 1$, the second terms in Eqs. (20) and (21) are estimated to be larger than $O(10^{-2})$, which is much larger than the SM values of those Yukawa coupling constants. In order to realize the Yukawa coupling constants compatible with the up- and down-quark masses, such contributions should be cancelled by $y_{u,d}(M_*)$, which requires a significant tuning between those two unrelated quantities.

For the scenario of isospin-violating DM, in fact, y_{U_L} and y_{D_L} may vanish; in order to generate the operator $\phi\phi\bar{q}q$, we only need y_{U_R} and y_{D_R} . They also affect the up- and down-quark Yukawa coupling constants. The contributions which are proportional to y_{U_R} and y_{D_R} are finite, and are given by

$$\Delta y_u = \frac{1}{8\pi^2} \lambda_Q \lambda_U y_{U_R} \frac{M_Q M_U}{M_Q^2 - M_U^2} \log \frac{M_U}{M_Q}, \quad (22)$$

$$\Delta y_d = \frac{1}{8\pi^2} \lambda_Q \lambda_U y_{D_R} \frac{M_Q M_D}{M_Q^2 - M_D^2} \log \frac{M_D}{M_Q}, \quad (23)$$

which are still much larger than the SM values of up- and down-quark Yukawa coupling constant if $\lambda_{Q,U,D} \sim y_{U_R,D_R} \sim 1$. Thus, the serious tunings of the counter terms of the Yukawa coupling constants are unavoidable in the present model.

4.2 Electric dipole moment of neutron

Next, we consider the electric dipole moment (EDM) of the neutron. If the newly introduced coupling constants have phases, which is the case in general, they become a new source of CP violations. In the present model, the DM sector necessarily couple to the first generation quarks, so the important check point is the neutron EDM.

In order to see how large the neutron EDM becomes, we calculate the coefficients of the EDM and chromo-EDM (CEDM) operators of up- and down-quarks:

$$\mathcal{L}_{(C)EDM} = \frac{i}{2} \sum_{f=u,d} \left[d_f F_{\mu\nu} \bar{f} \sigma_{\mu\nu} \gamma_5 f + g_3 \tilde{d}_f G_{\mu\nu}^{(a)} T_{\alpha\beta}^a \bar{f} \sigma_{\mu\nu} \gamma_5 f \right], \quad (24)$$

where $F_{\mu\nu}$ and $G_{\mu\nu}^{(a)}$ are field-strength tensors of photon and gluon, respectively, g_3 is the strong gauge coupling constant, and $T_{\alpha\beta}^a$ is the generator for $SU(3)_C$ (with α and β being

color indices, while a being index for the adjoint representation). With the (C)EDMs of quarks being given, the neutron EDM is estimated as [65]

$$d_n = -0.12d_u + 0.47d_d + e(-0.18\tilde{d}_u + 0.18\tilde{d}_d). \quad (25)$$

(The numerical uncertainties in QCD parameters may change the above formula by $\sim 10\%$ [65]. The conclusion of this subsection is, however, unaffected by such an uncertainty.)

As shown in the previous section, the LHC bounds require that the masses of the colored mediators should be much larger than the Higgs VEV, $M_{Q,U,D} > v$. In such a case, the coefficients of the (C)EDM operators can be expanded in powers of the Higgs VEV, and we only keep the leading-order terms in v . In the limit of $m_\phi \ll M_{Q,U,D}$ (with m_ϕ being the mass of the scalar DM) we obtain

$$d_u = \frac{1}{32\pi^2} \frac{eQ_U v}{M_Q M_U} \Im(\lambda_Q \lambda_U^* y_{U_R}), \quad (26)$$

$$\tilde{d}_u = \frac{1}{32\pi^2} \frac{v}{M_Q M_U} \Im(\lambda_Q \lambda_U^* y_{U_L}), \quad (27)$$

and d_d and \tilde{d}_d are obtained from d_u and \tilde{d}_u by replacing the subscripts as $U \rightarrow D$. Here, e is the electric charge, $Q_U = \frac{2}{3}$, and $Q_D = -\frac{1}{3}$. We note here that, at the leading order in v , the contribution proportional to $\Im(\lambda_Q \lambda_U^* y_{U_L})$ vanishes.

Taking $M_Q = M_U = M_D$ for simplicity, we obtain

$$d_n \simeq \left[-2.8 \times 10^{-21} e \text{ cm} \times \Im(\lambda_Q \lambda_U^* y_{U_R}) + 2.5 \times 10^{-22} e \text{ cm} \times \Im(\lambda_Q \lambda_D^* y_{D_R}) \right] \left(\frac{1 \text{ TeV}}{M_Q} \right)^2. \quad (28)$$

This should be compared with the present bound on the neutron EDM, which is given by [35]

$$|d_n| < 0.29 \times 10^{-25} e \text{ cm}. \quad (29)$$

Thus, the neutron EDM provides a very severe constraint on the complex phases of the couplings, $\Im(\lambda_Q \lambda_U^* y_{U_R}) \lesssim O(10^{-5} - 10^{-4})$ and $\Im(\lambda_Q \lambda_D^* y_{D_R}) \lesssim O(10^{-4} - 10^{-3})$, for $M_Q \simeq O(1 - 3) \text{ TeV}$.

4.3 $K-\bar{K}$ mixing

In the present analysis, we introduced only one set of vector-like fermions (i.e., Q , U , and D) for minimality. No symmetry forbids their interactions with second- and third-generation quarks. Such interactions in general induce unwanted CP and flavor violations; it is often the case that the $K-\bar{K}$ mixing parameters, i.e., ϵ_K and Δm_K , give stringent constraints. Thus, we consider them in this subsection.

The effective $\Delta S = 2$ Hamiltonian can be described as

$$\mathcal{H}_{\text{eff}} = \sum_{i=1}^3 (C_{L,i} \mathcal{Q}_{L,i} + C_{R,i} \mathcal{Q}_{R,i}) + \sum_{i=4}^5 C_i \mathcal{Q}_i, \quad (30)$$

where the operators are

$$\mathcal{Q}_{L,1} = (\bar{d}_\alpha \gamma_\mu P_L s_\alpha) (\bar{d}_\beta \gamma^\mu P_L s_\beta), \quad (31)$$

$$\mathcal{Q}_{L,2} = (\bar{d}_\alpha P_L s_\alpha) (\bar{d}_\beta P_L s_\beta), \quad (32)$$

$$\mathcal{Q}_{L,3} = (\bar{d}_\alpha P_L s_\beta) (\bar{d}_\beta P_L s_\alpha), \quad (33)$$

$$\mathcal{Q}_4 = (\bar{d}_\alpha P_L s_\alpha) (\bar{d}_\beta P_R s_\beta), \quad (34)$$

$$\mathcal{Q}_5 = (\bar{d}_\alpha P_L s_\beta) (\bar{d}_\beta P_R s_\alpha), \quad (35)$$

and $\mathcal{Q}_{R,i} = [\mathcal{Q}_{L,i}]_{L \rightarrow R}$. We calculate the Wilson coefficients in the present model. As in the case of neutron EDM, we use the mass-insertion approximation and only consider the leading contributions with respect to the insertions of the Higgs VEV.

In the case of real scalar DM, sum of the diagrams with no Higgs-VEV insertion vanishes, and the leading contributions are given by

$$C_{L,2}^{(\phi:\text{real})} = \frac{1}{16\pi^2} \frac{v^2}{M_Q^4} (\lambda_D^{s*} \lambda_Q^d)^2 [y_{D_R}^2 F_0(x_D, x_\phi) + y_{D_R} y_{D_L} F_1(x_D) + y_{D_L}^2 F_2(x_D)], \quad (36)$$

$$C_{R,2}^{(\phi:\text{real})} = \frac{1}{16\pi^2} \frac{v^2}{M_Q^4} (\lambda_Q^{s*} \lambda_D^d)^2 [y_{D_R}^{*2} F_0(x_D, x_\phi) + y_{D_R}^* y_{D_L}^* F_1(x_D) + y_{D_L}^{*2} F_2(x_D)], \quad (37)$$

$$C_4^{(\phi:\text{real})} = \frac{1}{8\pi^2} \frac{v^2}{M_Q^4} \lambda_Q^{s*} \lambda_D^{s*} \lambda_Q^d \lambda_D^d [y_{D_R} y_{D_R}^* F_0(x_D, x_\phi) + \Re(y_{D_R} y_{D_L}^*) F_1(x_D) + y_{D_L} y_{D_L}^* F_2(x_D)], \quad (38)$$

where

$$F_0(x_D, x_\phi) = -\frac{\log x_\phi}{x_D} + \frac{-2x_D^3 + 4x_D^2 - 4x_D + (3x_D - 1) \log x_D + 2}{(x_D - 1)^3 x_D}, \quad (39)$$

$$F_1(x_D) = \frac{-2x_D^2 + 4x_D \log x_D + 2}{\sqrt{x_D} (x_D - 1)^3}, \quad (40)$$

$$F_2(x_D) = \frac{-2x_D + (x_D + 1) \log x_D + 2}{(x_D - 1)^3}, \quad (41)$$

with $x_D \equiv M_D^2/M_Q^2$ and $x_\phi \equiv m_\phi^2/M_Q^2$. (The superscripts d and s of $\lambda_{Q,D}^{d,s}$ denote the coupling constants to the first and second generations, respectively, cf. Eq. (9).) Notice that the above expressions are valid only when $m_\phi \ll M_{Q,D}$. (Other Wilson coefficients

vanish at this order.) For complex scalar DM, we obtain

$$C_{L,1}^{(\phi:\text{complex})} = -\frac{1}{128\pi^2} \frac{1}{M_Q^2} (\lambda_Q^{s*} \lambda_Q^d)^2, \quad (42)$$

$$C_{R,1}^{(\phi:\text{complex})} = -\frac{1}{128\pi^2} \frac{1}{M_D^2} (\lambda_D^{s*} \lambda_D^d)^2, \quad (43)$$

$$C_{L,2}^{(\phi:\text{complex})} = \frac{1}{32\pi^2} \frac{v^2}{M_Q^4} (\lambda_Q^{s*} \lambda_Q^d)^2 [y_{D_R}^2 F_0(x_D, x_\phi) + y_{D_R} y_{D_L} F_1(x_D) + y_{D_L}^2 F_2(x_D)], \quad (44)$$

$$C_{R,2}^{(\phi:\text{complex})} = \frac{1}{32\pi^2} \frac{v^2}{M_Q^4} (\lambda_Q^{s*} \lambda_D^d)^2 [y_{D_R}^{*2} F_0(x_D, x_\phi) + y_{D_R}^* y_{D_L}^* F_1(x_D) + y_{D_L}^{*2} F_2(x_D)], \quad (45)$$

$$C_4^{(\phi:\text{complex})} = \frac{1}{16\pi^2} \frac{v^2}{M_Q^4} \lambda_Q^{s*} \lambda_D^{s*} \lambda_Q^d \lambda_D^d [y_{D_R} y_{D_R}^* F_0(x_D, x_\phi) + \Re(y_{D_R} y_{D_L}^*) F_1(x_D) + y_{D_L} y_{D_L}^* F_2(x_D)], \quad (46)$$

$$C_5^{(\phi:\text{complex})} = \frac{1}{16\pi^2} \lambda_Q^{s*} \lambda_D^{s*} \lambda_Q^d \lambda_D^d \frac{1}{M_Q^2 - M_D^2} \log \frac{M_Q}{M_D}, \quad (47)$$

where we neglected the terms which are higher order in v . (Other Wilson coefficients vanish at this order.)

With the Wilson coefficients, we calculate the matrix elements relevant for the study of K - \bar{K} mixing parameters. Here, our purpose is to obtain semi-quantitative bounds on the model parameters, so we use the vacuum-insertion approximation to evaluate the matrix elements. Then, we obtain [66]

$$\begin{aligned} \langle K | \mathcal{H}_{\text{eff}} | \bar{K} \rangle &= \frac{2}{3} (m_K f_K)^2 (C_{L,1} + C_{R,1}) - \frac{5}{12} \frac{m_K^2}{m_s^2} (m_K f_K)^2 (C_{L,2} + C_{R,2}) \\ &+ \frac{1}{12} \frac{m_K^2}{m_s^2} (m_K f_K)^2 (C_{L,3} + C_{R,3}) + \left(\frac{1}{12} + \frac{1}{2} \frac{m_K^2}{m_s^2} \right) (m_K f_K)^2 C_4 \\ &+ \left(\frac{1}{4} + \frac{1}{6} \frac{m_K^2}{m_s^2} \right) (m_K f_K)^2 C_5, \end{aligned} \quad (48)$$

where m_K is the mass of K , $m_s \simeq 95$ MeV is the strange-quark mass, and $f_K \simeq 160$ MeV is the decay constant. With the above matrix element, we estimate the DM sector contributions to the K - \bar{K} mixing parameters as

$$|\epsilon_K^{(\phi)}| = \frac{\Im \langle K | \mathcal{H}_{\text{eff}} | \bar{K} \rangle}{2\sqrt{2} m_K \Delta m_K}, \quad (49)$$

$$\Delta m_K^{(\phi)} = \frac{1}{m_K} |\langle K | \mathcal{H}_{\text{eff}} | \bar{K} \rangle|. \quad (50)$$

The numerical values of $\epsilon_K^{(\phi)}$ and $\Delta m_K^{(\phi)}$ depend on various parameters. Taking

$$\lambda_Q^s = \lambda_D^2 \equiv \lambda^s, \quad (51)$$

$$y_{D_L} = y_{D_R} \equiv y_D, \quad (52)$$

as well as the relations given in Eqs. (11) – (14), for example, we obtain

$$|\epsilon_K^{(\phi:\text{real})}| \simeq 6.5 \times 10^3 \times \Im(\lambda^{s*}\lambda^d)^2 y_D^2 \left(\frac{1 \text{ TeV}}{M}\right)^4 \left[1 + 0.34 \log \frac{(M/m_\phi)}{100}\right], \quad (53)$$

and

$$|\epsilon_K^{(\phi:\text{complex})}| \simeq 1.7 \times 10^4 \times \Im(\lambda^{s*}\lambda^d)^2 \left(\frac{1 \text{ TeV}}{M}\right)^2 + 3.2 \times 10^3 \times \Im(\lambda^{s*}\lambda^d)^2 y_D^2 \left(\frac{1 \text{ TeV}}{M}\right)^4 \left[1 + 0.34 \log \frac{(M/m_\phi)}{100}\right], \quad (54)$$

for the cases where ϕ is real and complex, respectively. (Here, we assumed that y_D is real for simplicity.) In addition, with the present choice of parameters,

$$\Delta m_K^{(\phi)} \simeq 1.5 \times 10^{10} \text{ sec}^{-1} \times \frac{|\lambda^{s*}\lambda^d|^2}{\Im(\lambda^{s*}\lambda^d)^2} |\epsilon_K^{(\phi)}|. \quad (55)$$

The measured values of the K - \bar{K} mixing parameters are well explained by the SM, and there exist stringent constraints on the extra contributions to those quantities. Comparing the SM prediction ($\epsilon_K^{(\text{SM})} = (1.81 \pm 0.28) \times 10^{-3}$ [67]) and the experimental value ($\epsilon_K^{(\text{exp})} = (2.228 \pm 0.011) \times 10^{-3}$ [35]), the DM sector contribution to ϵ_K is constrained to be $|\epsilon_K^{(\phi)}| < 9.8 \times 10^{-4}$. In addition, the experimental value of Δm_K is known to be $\Delta m_K^{(\text{exp})} = (0.5293 \pm 0.0009) \times 10^{10} \text{ sec}^{-1}$ [35], which we use as an upper bound on $\Delta m_K^{(\phi)}$. Assuming no accidental cancellation among contributions from different Feynman diagrams, the DM sector contributions are likely to become much larger than the upper bounds on those quantities unless some of the coupling constants are much smaller than 1, as indicated by Eqs. (53) – (55).

5 Conclusion

In this paper, we have studied isospin-violating light DM that can explain the possible CDMS-Si signal of light DM, while avoiding the constraints by recent LUX and SuperCDMS experiments. In particular, we considered isospin-violating light DM models with colored mediators. We have shown that a minimal viable model includes scalar DM and new colored vector-like fermions with masses of $O(1)$ TeV as mediators. We investigated the collider searches, flavor and CP phenomenology. The masses of colored mediators are constrained by the 8 TeV LHC results as $M \gtrsim 1 - 1.5 \text{ TeV}$ ($1 - 1.1 \text{ TeV}$) for real (complex) scalar DM. The 14 TeV LHC may cover a large region of the remaining parameter space.

We have also studied flavor and CP constraints on the colored-mediator model for the isospin-violating DM. In such a model, the interaction of quarks with colored mediator and DM should be sizable, which results in large radiative correction to flavor and CP

observables. We have studied the effects on the quark masses (in particular, those of up- and down-quarks), EDM of neutron, and the K - \bar{K} mixing parameters. Radiative corrections to the SM Yukawa couplings from the DM sector are extremely large, and hence fine-tunings are unavoidable. Flavor and CP violating observables also impose severe constraints on the present scenario.

Acknowledgment

This work was supported by JSPS KAKENHI Grant No. 22244021 (K.H., T.M.), No. 22540263 (T.M.), No. 23104008 (T.M.) and also by World Premier International Research Center Initiative (WPI Initiative), MEXT, Japan. The work of S.P.L. was supported by the Program for Leading Graduate Schools, MEXT, Japan. The work of Y.Y. has been supported in part by the Ministry of Economy and Competitiveness (MINECO), grant FPA2010-17915, and by the Junta de Andalucía, grants FQM 101 and FQM 6552.

A Isospin–Violating Fermionic Dark Matter with Colored Scalar Mediators

In this appendix, we briefly discuss isospin–violating fermionic DM models with colored scalar mediators. The effective operators $\mathcal{O}^{(M)}$ and $\mathcal{O}^{(Ds)}$ in Table 1 can be induced by exchanges of colored scalars \tilde{Q}_L , \tilde{Q}_R with the following Lagrangian:

$$L \supset y_L \chi_{qL} \tilde{Q}_L + y_R \chi_{qR} \tilde{Q}_R + AH \tilde{Q}_L^* \tilde{Q}_R. \quad (56)$$

The benchmark point in Eq. (6), when interpreted with this Lagrangian, corresponds to

$$C^{(M)} \simeq \frac{y_L y_R A v}{2m_{\tilde{Q}}^4} \simeq \frac{1}{(1.05 \text{ TeV})^2}, \quad (57)$$

$$C^{(Ds)} \simeq \frac{y_L y_R A v}{4m_{\tilde{Q}}^4} \simeq \frac{1}{(1.05 \text{ TeV})^2}, \quad (58)$$

where we assume all colored scalars have common mass $m_{\tilde{Q}}$. Assuming that $y_L, y_R \lesssim 1$, and $A \lesssim m_{\tilde{Q}}$ for perturbative unitarity condition, the colored scalar mass parameter should be smaller than 460 GeV (360 GeV) for Majorana (Dirac) DM.

If the colored scalar is produced at the LHC, it will decay into a SM quark and DM. This collider signature is analogous to that of SUSY models with almost massless neutralino and a very heavy gluino. Such a simplified SUSY model is searched for at the LHC, and the lower limit on the mass of squark is 780 GeV [63]. The limit can be directly applied to the current setup, since squark pairs are mainly produced by QCD processes in both models. Hence, as an explanation of the CDMS-Si signal, isospin–violating fermionic DM models with colored scalar mediators are already disfavored by current LHC results.

References

- [1] P. A. R. Ade *et al.* [Planck Collaboration], arXiv:1303.5076 [astro-ph.CO].
- [2] For a review, see, for example, G. Bertone, D. Hooper and J. Silk, Phys. Rept. **405** (2005) 279 [hep-ph/0404175].
- [3] R. Bernabei *et al.* [DAMA and LIBRA Collaborations], Eur. Phys. J. C **67** (2010) 39 [arXiv:1002.1028 [astro-ph.GA]].
- [4] C. E. Aalseth *et al.* [CoGeNT Collaboration], Phys. Rev. Lett. **106** (2011) 131301 [arXiv:1002.4703 [astro-ph.CO]].
- [5] C. E. Aalseth, P. S. Barbeau, J. Colaresi, J. I. Collar, J. Diaz Leon, J. E. Fast, N. Fields and T. W. Hossbach *et al.*, Phys. Rev. Lett. **107** (2011) 141301 [arXiv:1106.0650 [astro-ph.CO]].
- [6] C. E. Aalseth *et al.* [CoGeNT Collaboration], arXiv:1401.3295 [astro-ph.CO].
- [7] G. Angloher, M. Bauer, I. Bavykina, A. Bento, C. Bucci, C. Ciemniak, G. Deuter and F. von Feilitzsch *et al.*, Eur. Phys. J. C **72** (2012) 1971 [arXiv:1109.0702 [astro-ph.CO]].
- [8] R. Agnese *et al.* [CDMS Collaboration], [arXiv:1304.4279 [hep-ex]].
- [9] J. Angle *et al.* [XENON10 Collaboration], Phys. Rev. Lett. **107** (2011) 051301 [arXiv:1104.3088 [astro-ph.CO]].
- [10] E. Aprile *et al.* [XENON100 Collaboration], Phys. Rev. Lett. **109** (2012) 181301 [arXiv:1207.5988 [astro-ph.CO]].
- [11] D. S. Akerib *et al.* [LUX Collaboration], arXiv:1310.8214 [astro-ph.CO].
- [12] M. Felizardo, T. A. Girard, T. Morlat, A. C. Fernandes, A. R. Ramos, J. G. Marques, A. Kling and J. Puibasset *et al.*, Phys. Rev. Lett. **108** (2012) 201302 [arXiv:1106.3014 [astro-ph.CO]].
- [13] D. S. Akerib *et al.* [CDMS Collaboration], Phys. Rev. D **82** (2010) 122004 [arXiv:1010.4290 [astro-ph.CO]].
- [14] Z. Ahmed *et al.* [CDMS-II Collaboration], Phys. Rev. Lett. **106** (2011) 131302 [arXiv:1011.2482 [astro-ph.CO]].
- [15] R. Agnese *et al.* [SuperCDMS Soudan Collaboration], Phys. Rev. Lett. [Phys. Rev. Lett. **112** (2014) 041302] [arXiv:1309.3259 [physics.ins-det]].
- [16] R. Agnese *et al.* [SuperCDMS Collaboration], arXiv:1402.7137 [hep-ex].

- [17] M. I. Gresham and K. M. Zurek, Phys. Rev. D **89** (2014) 016017 [arXiv:1311.2082 [hep-ph]].
- [18] E. Del Nobile, G. B. Gelmini, P. Gondolo and J. -H. Huh, arXiv:1311.4247 [hep-ph].
- [19] P. J. Fox, G. Jung, P. Sorensen and N. Weiner, arXiv:1401.0216 [hep-ph].
- [20] A. Kurylov and M. Kamionkowski, Phys. Rev. D **69** (2004) 063503 [hep-ph/0307185].
- [21] F. Giuliani, Phys. Rev. Lett. **95** (2005) 101301 [hep-ph/0504157].
- [22] S. Chang, J. Liu, A. Pierce, N. Weiner and I. Yavin, JCAP **1008** (2010) 018 [arXiv:1004.0697 [hep-ph]].
- [23] Z. Kang, T. Li, T. Liu, C. Tong and J. M. Yang, JCAP **1101** (2011) 028 [arXiv:1008.5243 [hep-ph]].
- [24] J. L. Feng, J. Kumar, D. Marfatia and D. Sanford, Phys. Lett. B **703** (2011) 124 [arXiv:1102.4331 [hep-ph]].
- [25] M. T. Frandsen, F. Kahlhoefer, C. McCabe, S. Sarkar and K. Schmidt-Hoberg, JCAP **1307** (2013) 023 [arXiv:1304.6066 [hep-ph]].
- [26] J. L. Feng, J. Kumar and D. Sanford, Phys. Rev. D **88** (2013) 015021 [arXiv:1306.2315 [hep-ph]].
- [27] V. Cirigliano, M. L. Graesser, G. Ovanesyan and I. M. Shoemaker, arXiv:1311.5886 [hep-ph].
- [28] S. Chang, R. Edezhath, J. Hutchinson and M. Luty, arXiv:1307.8120 [hep-ph].
- [29] H. An, L. -T. Wang and H. Zhang, arXiv:1308.0592 [hep-ph].
- [30] Y. Bai and J. Berger, JHEP **1311** (2013) 171 [arXiv:1308.0612 [hep-ph]].
- [31] A. DiFranzo, K. I. Nagao, A. Rajaraman and T. M. P. Tait, JHEP **1311** (2013) 014 [arXiv:1308.2679 [hep-ph]].
- [32] M. Papucci, A. Vichi and K. M. Zurek, arXiv:1402.2285 [hep-ph].
- [33] M. R. Buckley and W. H. Lippincott, Phys. Rev. D **88** (2013) 056003 [arXiv:1306.2349 [hep-ph]].
- [34] J. R. Ellis, K. A. Olive and C. Savage, Phys. Rev. D **77** (2008) 065026 [arXiv:0801.3656 [hep-ph]].
- [35] J. Beringer *et al.* [Particle Data Group Collaboration], Phys. Rev. D **86** (2012) 010001.

- [36] A. Birkedal, K. Matchev and M. Perelstein, Phys. Rev. D **70** (2004) 077701 [hep-ph/0403004].
- [37] M. Beltran, D. Hooper, E. W. Kolb, Z. A. C. Krusberg and T. M. P. Tait, JHEP **1009**, 037 (2010) [arXiv:1002.4137 [hep-ph]].
- [38] J. Goodman, M. Ibe, A. Rajaraman, W. Shepherd, T. M. P. Tait and H. -B. Yu, Phys. Lett. B **695**, 185 (2011) [arXiv:1005.1286 [hep-ph]].
- [39] J. Goodman, M. Ibe, A. Rajaraman, W. Shepherd, T. M. P. Tait and H. -B. Yu, Phys. Rev. D **82** (2010) 116010 [arXiv:1008.1783 [hep-ph]].
- [40] Y. Bai, P. J. Fox and R. Harnik, JHEP **1012** (2010) 048 [arXiv:1005.3797 [hep-ph]].
- [41] P. J. Fox, R. Harnik, J. Kopp and Y. Tsai, Phys. Rev. D **84**, 014028 (2011) [arXiv:1103.0240 [hep-ph]].
- [42] P. J. Fox, R. Harnik, J. Kopp and Y. Tsai, Phys. Rev. D **85** (2012) 056011 [arXiv:1109.4398 [hep-ph]].
- [43] Y. Bai and T. M. P. Tait, Phys. Lett. B **723** (2013) 384 [arXiv:1208.4361 [hep-ph]].
- [44] S. Chatrchyan *et al.* [CMS Collaboration], arXiv:1206.5663 [hep-ex].
- [45] [CMS Collaboration], CMS-PAS-EXO-12-048.
- [46] S. Chatrchyan *et al.* [CMS Collaboration], arXiv:1204.0821 [hep-ex].
- [47] [CMS Collaboration], CMS-PAS-EXO-13-004.
- [48] G. Aad *et al.* [ATLAS Collaboration], JHEP **1304** (2013) 075 [arXiv:1210.4491 [hep-ex]].
- [49] [ATLAS Collaboration], ATLAS-CONF-2012-147.
- [50] G. Aad *et al.* [ATLAS Collaboration], arXiv:1309.4017 [hep-ex].
- [51] J. Alwall, M. Herquet, F. Maltoni, O. Mattelaer and T. Stelzer, JHEP **1106** (2011) 128 [arXiv:1106.0522 [hep-ph]].
- [52] J. Kumar, D. Sanford and L. E. Strigari, Phys. Rev. D **85** (2012) 081301 [arXiv:1112.4849 [astro-ph.CO]].
- [53] A. Friedland, M. L. Graesser, I. M. Shoemaker and L. Vecchi, Phys. Lett. B **714** (2012) 267 [arXiv:1111.5331 [hep-ph]].
- [54] I. M. Shoemaker and L. Vecchi, Phys. Rev. D **86** (2012) 015023 [arXiv:1112.5457 [hep-ph]].

- [55] G. Busoni, A. De Simone, E. Morgante and A. Riotto, arXiv:1307.2253 [hep-ph].
- [56] O. Buchmueller, M. J. Dolan and C. McCabe, JHEP **1401** (2014) 025 [arXiv:1308.6799 [hep-ph], arXiv:1308.6799].
- [57] M. Ackermann *et al.* [Fermi-LAT Collaboration], Phys. Rev. Lett. **107** (2011) 241302 [arXiv:1108.3546 [astro-ph.HE]].
- [58] A. Geringer-Sameth and S. M. Koushiappas, Phys. Rev. Lett. **107** (2011) 241303 [arXiv:1108.2914 [astro-ph.CO]].
- [59] M. Ackermann *et al.* [Fermi-LAT Collaboration], Phys. Rev. D **89** (2014) 042001 [arXiv:1310.0828 [astro-ph.HE]].
- [60] X. -G. He and J. Tandean, Phys. Rev. D **88** (2013) 013020 [arXiv:1304.6058 [hep-ph]].
- [61] N. Okada and O. Seto, Phys. Rev. D **88** (2013) 063506 [arXiv:1304.6791 [hep-ph]].
- [62] G. Belanger, A. Goudelis, J. -C. Park and A. Pukhov, arXiv:1311.0022 [hep-ph].
- [63] The ATLAS collaboration, ATLAS-CONF-2013-047.
- [64] T. Cohen, T. Golling, M. Hance, A. Henrichs, K. Howe, J. Loyal, S. Padhi and J. G. Wacker, arXiv:1311.6480 [hep-ph].
- [65] J. Hisano, J. Y. Lee, N. Nagata and Y. Shimizu, Phys. Rev. D **85** (2012) 114044 [arXiv:1204.2653 [hep-ph]].
- [66] See, for example, A. J. Buras, S. Jager and J. Urban, Nucl. Phys. B **605** (2001) 600 [hep-ph/0102316].
- [67] J. Brod and M. Gorbahn, Phys. Rev. Lett. **108** (2012) 121801.